Case Studies in Construction Materials 21 (2024) e03900

Contents lists available at ScienceDirect

Case Studies in Construction Materials

journal homepage: www.elsevier.com/locate/cscm

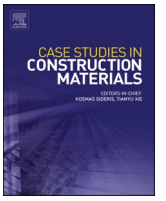

Experimental and numerical evaluation of sustainable application of steel slag as an alternative to gravel in compaction piles

Boyoung Yoon [a], Yonghun Cho [b], Hyunwook Choo [b,*], Jaewon Jang [c]

[a] School of Civil and Environmental Engineering Georgia Institute of Technology Atlanta, GA 30332, USA
[b] Department of Civil and Environmental Engineering, Hanyang University, Seoul 04763, South Korea
[c] Research Institute of Industrial Science & Technology, Pohang 37673, South Korea

ARTICLE INFO

Keywords:
Steel slag
Compaction pile
Gravel
Soil improvement
Cementation
SPT

ABSTRACT

The study investigates the application of steel slag as an innovative material for compaction piles in the stabilization of soft soils, offering an eco-friendly alternative to conventional gravel compaction piles (GCPs). Through a comprehensive series of laboratory tests, field experiments, and numerical simulations, this study evaluated the performance, environmental impact, and long-term behavior of steel slag compaction piles (SSCPs). The key findings revealed that steel slag not only provides immediate soil improvement comparable to gravel but also exhibits significant time-dependent increases in strength and stiffness. Standard Penetration Test (SPT) *N*-ratios (N_1/N_0, where $N_1 = N$ value after improvement and $N_0 = N$ value before improvement) were similar for soils reinforced with SSCPs and GCPs after 0 months, but were about 30 % higher in SSCP-reinforced soils after 3 months. This increase was attributed to the cementation of steel slags, suggesting that the compaction pile with increased stiffness due to cementation acts as a compaction pile with an increased area replacement ratio (α). Environmental assessments confirmed that steel slag meets regulatory standards for soil contamination, positioning it as a sustainable option. Settlement analysis after embankment construction showed reduced and more uniform settlements with SSCPs, suggesting superior load distribution capabilities. Finite element analysis compared the behavior of SSCP-reinforced soils at varying α and stiffness of compaction piles, confirming that the cementation of steel slag produces an effect equivalent to increasing α in uncemented piles, thus enhancing the reinforcement effect.

1. Introduction

Rapid growth in the global population and the expansion of urban areas have increased the demand for essential infrastructure, such as buildings, roads, tunnels, and bridges. However, because areas with high-quality soil are already occupied by existing structures, civil engineers must confront the challenges posed by problematic soils with low bearing capacities and high compressibility in upcoming construction projects. Therefore, the focus has shifted towards ground improvement techniques that render these problematic soils suitable for construction. These techniques include preloading, dredging, and soil replacement [1,2].

Among the various methods, the granular or stone column method has gained popularity owing to its relative freedom from environmental restrictions and lower post-construction maintenance costs compared with other methods [3,4]. This method involves

* Corresponding author.
E-mail address: choohw@hanyang.ac.kr (H. Choo).

https://doi.org/10.1016/j.cscm.2024.e03900
Received 23 August 2024; Received in revised form 15 October 2024; Accepted 20 October 2024
Available online 22 October 2024

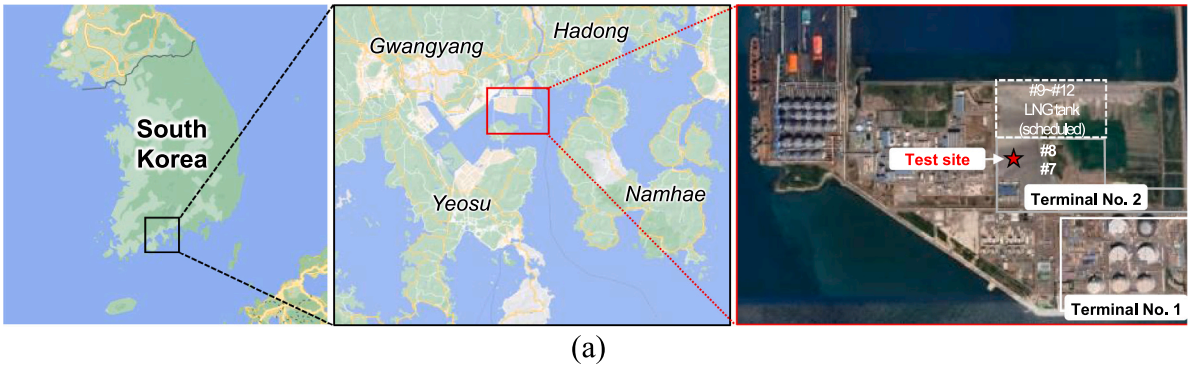

(a)

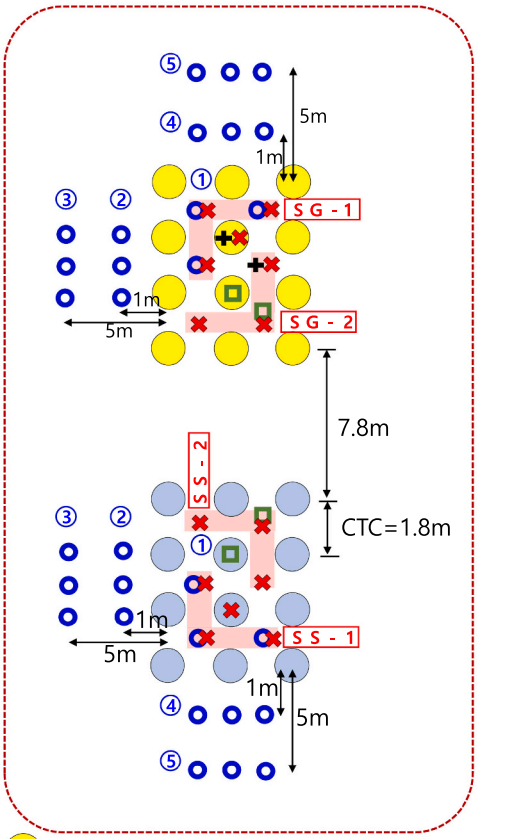

GCP: Gravel Compaction Pile

SSCP: Steel Slag Compaction Pile

Standard penetration test (SPT)

Plate load test (PLT)

Soil sampling for environmental assessment

Note: CTC = pile center – to- center distance

(b)

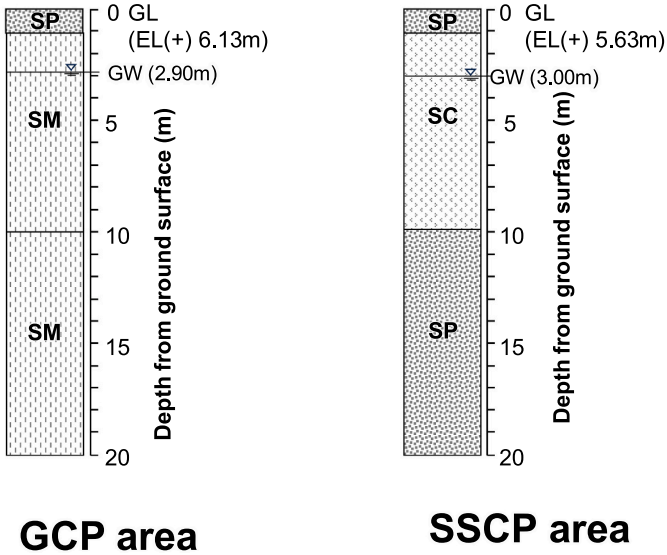

(c)

Fig. 1. (a) The location of test site, (b) pile arrangements and field test locations, and (c) drill-log of subsoil before pile construction.

replacing weak soil with coarse granular materials such as sand and gravel, creating a vertical element that is stiffer and stronger than the surrounding soil. The resulting composite ground, comprising a granular column and in-situ soil with enhanced engineering properties through densification, is known to reduce the total and differential settlement of foundations and improve the bearing capacity of soils [3,5,6]. Commonly, a granular (or vertical) column is filled with compacted sand or gravel or stone; these are called the sand compaction pile (SCP) method or the gravel compaction pile (GCP) method, respectively. However, the global scarcity of natural aggregates has hindered the widespread application of SCP and GCP. Consequently, there has been a growing interest in recycled aggregates for sustainable practices [7,8]. Specifically, materials such as steel slag, spent railway ballast, crushed concrete, demolition materials, and waste rock have gained attention owing to their potential use as construction materials [9].

Steel slag is a solid waste generated from both steelmaking and refining operations and has a wide size distribution ranging from gravel-sized particles to silt-sized particles. Steel slag exhibits very high shear strength owing to its angular particle shape, characterized by distinct asperities and sharp edges, and its mineral composition [10]. Additionally, steel slag is a weak cementitious material because it contains low levels of tricalcium silicates (C_3S, Ca_3SiO_5, alite) [11]. Rapid and massive growth in steel demand has resulted in a steady increase in steel slag generation. It is estimated that approximately 190–280 million tons of steel slag were generated globally in 2021 [12]. In South Korea, approximately 10 million tons of steel slag is generated every year [13]. While steel slag is partially reused as fill material [14,15], asphalt paving [16], and road bases [17], there remains a substantial portion, approximately 60 %, of the slag generated worldwide, which still requires effective reuse strategies.

Recently, efforts have been made to utilize the coarse particle characteristics of steel slag as newly-developed aggregates for granular columns. Several studies have demonstrated the ground improvement effect of steel slag compaction piles (SSCPs) by employing laboratory tests, such as large-scale direct shear tests [18] and California bearing tests [19], on composite soils with SSCPs. However, only a few studies conducted field tests to demonstrate the applicability of steel slag as a granular column and its effectiveness in ground improvement [20]. Moreover, the effect of the time-dependent strength gain of steel slag due to cementation on the composite ground behavior and the environmental impact of SSCP has rarely been studied.

This study aimed to assess the feasibility of using steel slag produced at POSCO in South Korea as aggregates for compaction piles, replacing 100 % of the natural aggregates in the piles. Researchers have conducted a series of field and laboratory tests to evaluate the performance of SSCPs in comparison with traditional GCPs. For the field tests, groups of GCPs and SSCPs were constructed adjacent to each other, and Standard Penetration Tests (SPT) and Plate Load Tests (PLT) were performed on the granular columns and in-situ soils before and after pile construction. The settlement of the composite ground was also monitored over a three-month period following the construction of a 2-meter-high embankment. Furthermore, the environmental impact of the fill materials (or aggregates) and their effects on soil contamination were evaluated. In the laboratory, shear wave velocity measurement tests were conducted on steel slag and gravel. To further enhance the evaluation, this study included a numerical assessment of the footing performance of composite soils with SSCPs at varying replacement ratios and elastic moduli. Comprehensive comparative analyses between GCPs and SSCPs aimed to provide insights into the feasibility of using steel slag as a viable fill material for granular columns.

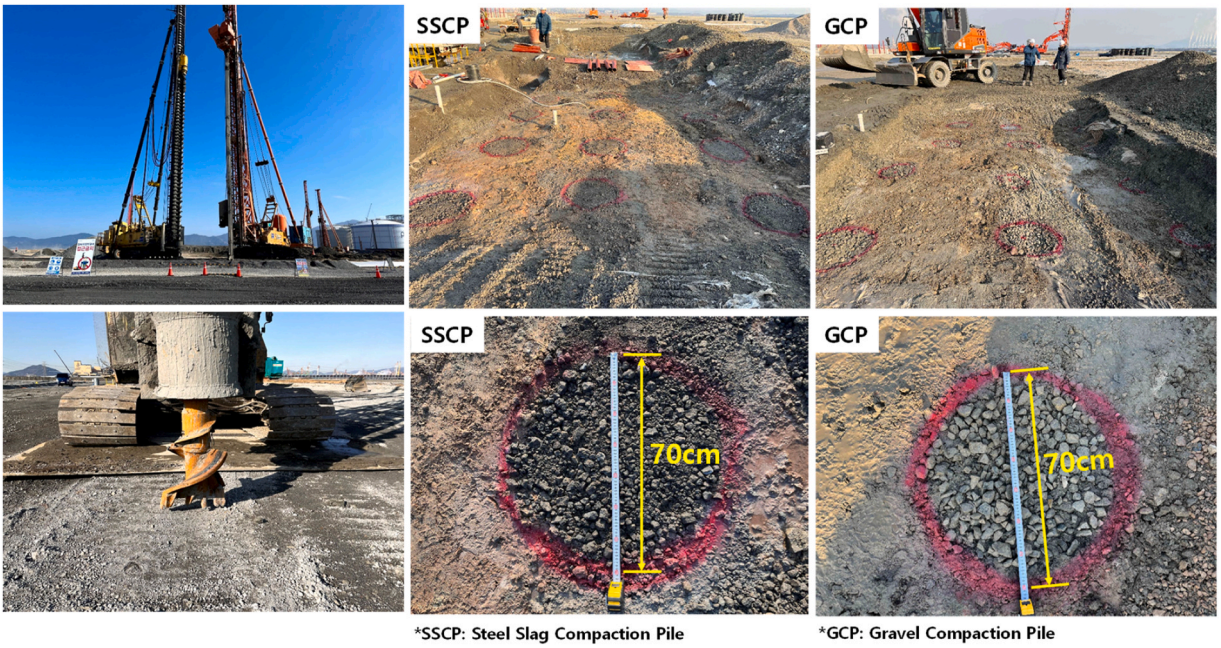

Fig. 2. The overview of compaction pile installation.

2. Experimental program

2.1. Test sites and compaction pile installation

The test site is located in the southern part of South Korea, specifically in the northern area of the Gwangyang LNG Terminal (Jeollanam-do, South Korea), as shown in Fig. 1(a). This study investigated the feasibility of using steel slag as a full replacement for natural aggregates in compaction piles. Thus, gravel compaction piles (GCPs) and steel slag compaction piles (SSCPs) were constructed adjacent to each other at a distance of 7.8 m between them (Fig. 1(b)). Both the GCPs and SSCPs were arranged in a grid formation of three rows and four columns. Each pile had a diameter of 0.7 m and a spacing of 1.8 m, with a target length of 20 m. The area replacement ratio (α), calculated as the ratio of the sectional area of the compaction piles to the total area of both the compaction piles and surrounding soils [21], was 12 %. Note that $\alpha < 30$ % is considered a low α [22].

Fig. 1(c) shows the drill logs of the in-situ soil before the construction of the GCPs and SSCPs. This reveals that both sites typically possess a thin layer of poorly graded sandy soil. Beneath this, a silty sand layer was identified at the GCP construction sites, whereas clayey sand was found at the SSCP construction sites. Before ground modification, these in-situ soils were determined to be in a loose to moderately dense state based on the Standard Penetration Test (SPT) results, which will be discussed later. The water level at both sites was approximately 3.0 m deep.

The construction sequence of the compaction piles involved inserting a casing with a diameter of 0.4 m into the ground to the desired soil improvement depth and then filling the casing with gravel or steel slag. Afterward, the casing is pulled up vertically by 3 m and re-driven by 2 m, forming a compaction pile with a diameter of 0.7 m and a height of 1 m. Fig. 2 shows the equipment used during pile installation and provides an overview of the constructed compaction piles. The diameters of the piles were confirmed via direct observation.

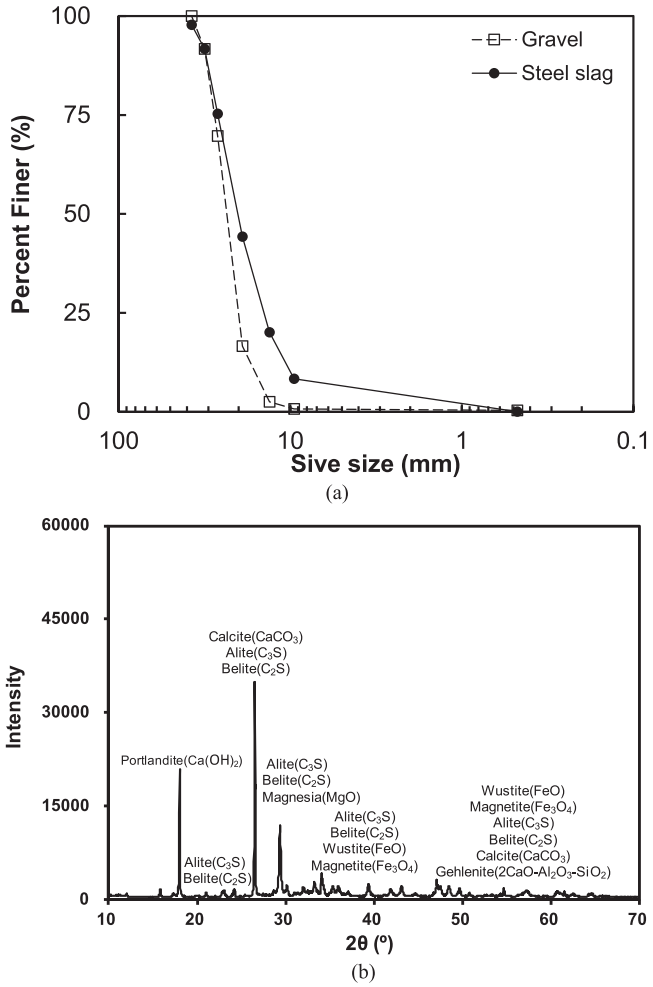

Fig. 3. (a) Particle size distribution of steel slag and gravel used in this study and (b) X-ray diffraction (XRD) pattern of steel slag.

2.2. Field surveys and methodologies

Fig. 1(b) details the location of comprehensive field tests, including SPT and Plate Load Test (PLT) conducted on the in-situ soils between compaction piles (inter-pile SPT and PLT) and on the compaction piles (in-pile SPT and PLT), both before and immediately after pile installation. The settlement of the composite ground was monitored for 3 months following the construction of a 2-m-high embankment. Subsequently, additional SPT was conducted on both the in-situ soils and compaction piles. Note that the PLT results were used to validate the numerical models, which aimed to evaluate the impact of α.

To evaluate the potential environmental impacts of the steel slag leachate, the leaching characteristics of the fill materials used in the compaction piles were analyzed according to Korean standards (ES 06000, Korea), and soil contamination by the compaction piles was assessed according to Korean standard ES 07000. For the soil contamination evaluation, the heavy metal content in soils was measured at distances of 1 m and 5 m and depths of 5 m and 15 m from the compaction pile (Fig. 1(b)) at three different time periods: immediately after compaction pile installation and 2 and 4 months after installation. Contaminant component analysis included 10 of the 22 soil contaminants specified in the enforcement rules for the Soil Environment Conservation Act of South Korea, excluding organic compounds such as phenols. The standard value for 'Region 1' was used to evaluate the contaminants. 'Region 1' applies to areas used for residential purposes, such as school grounds, fishponds, parks, historic sites, cemeteries, and outdoor children's playground facilities according to enforcement rules for the Soil Environment Conservation Act of South Korea.

2.3. Fill materials

The used compaction materials were obtained from local aggregate providers: gravels provided by Doo Won Industry Inc (Suncheon, Jeollanam-do, South Korea) and steel slags produced at POSCO Gwangyang steel mill (South Korea). Both the gravel and steel slag were sieved to obtain particles smaller than 40 mm to avoid blockage in the vibro-flotation machine [23]. The particle sizes of both materials ranged from 0.5 mm to 40 mm, as shown in Fig. 3(a). The median particle size (D_{50}) of the steel slag was determined to be 20.4 mm, and that of the gravel was 23.8 mm. Both materials exhibited poorly graded grain size distributions, with uniformity coefficients (C_u) of 1.45 for gravel and 2.11 for steel slag. The specific gravity (G_s) of the steel slag was 3.64, which notably exceeded that of gravel (= 2.59) and was attributed to the higher iron content in the steel slag. Table 1 lists the chemical compositions of the tested steel slag.

The steel slag generally contains a small amount of free CaO and MgO, which hydrate into calcium hydroxide ($Ca(OH)_2$) and magnesium hydroxide ($Mg(OH)_2$), respectively. This hydration process involves the volumetric expansion of steel slag, which is the primary cause of its limited application in engineering practice [24–27]. Thus, to minimize the volume instability of steel slag, the slag used in this study was subjected to wet aging (i.e., spraying water daily to promote hydration reactions) for one month, and Fig. 3(b) shows the X-ray diffraction (XRD) images of the steel slag after the wet aging. Due to the aging process, the hydration products of CaO, such as $Ca(OH)_2$ and $CaCO_3$, can be found in Fig. 3(b). However, the aging period was relatively short in this study; thus, the free swelling of steel slag was examined according to KS F 2580 [28]. The determined maximum swelling strain was approximately 1.2 % (Fig. S1 in supplementary material), indicating the insignificant volume expansion of the tested steel slag and the consequent possible use as an alternative to natural aggregates.

2.4. Laboratory test

To investigate the time-dependent stiffness or strength gain of the steel slag due to cementation, a bender element test was conducted within a large-scale oedometer cell using a cylindrical specimen with a diameter of 29.5 cm and a height of 20 cm (Fig. 4(a)). A pair of bender elements were embedded horizontally, one acting as a transmitter and the other as a receiver. The transmitter was excited with a square wave with a frequency of 20 Hz and an amplitude of 20 V, generated by a function generator (Keysight 33210 A) and a linear amplifier (Piezo Systems EPA-104). The receiver, which detected the signal traveling through the specimen, was connected to a filter/amplifier that was connected to a digital oscilloscope (Keysight DSOX 2014A).

Steel slag was prepared under optimum conditions (maximum dry unit weight = 21 kN/m^3 and optimum water content = 4 %), and the compacted specimen was inundated with deionized water under a vertical effective stress of 10 kPa. The shear wave velocity (V_s) evolution of the steel slag under a constant vertical effective stress of 10 kPa was measured as a function of time. For comparison, an identical test was performed using gravel specimens of the same dimensions under identical conditions, enabling a direct evaluation of the time-dependent stiffness evolution between the two materials.

Table 1
Chemical composition of tested steel slag (%)

MgO	Al_2O_3	SiO_2	P_2O_5	SO_3	Na2O	Cl	K_2O	CaO	TiO_2	V_2O_5	Cr_2O_3	MnO	Fe_2O_3
3.31	3.31	16.10	2.65	0.11	0.15	1.01	0.08	32.20	0.94	0.30	0.19	3.67	35.90

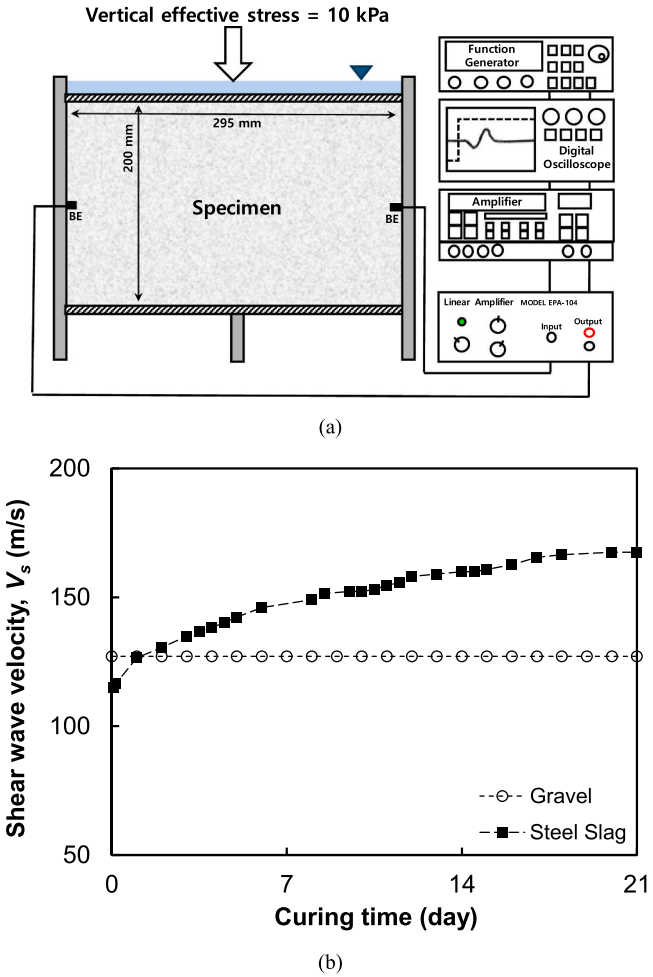

Fig. 4. (a) Test setup for shear wave velocity (V_s) measurement and (b) the variation of V_s according to time.

3. Experimental results and analysis

3.1. Laboratory test (shear wave velocity measurements)

Because steel slag can exhibit a time-dependent strength or stiffness gain owing to the hydration process, this study presents the shear wave velocity (V_s) of the tested steel slag as a function of time. For comparison, the result for gravel is also presented in this section.

Fig. 4(b) shows the V_s values of the two materials as functions of time. For the tested steel slag, V_s increased with time, approaching an asymptotic value after 18 days of curing. In contrast, the tested gravel showed an almost constant V_s regardless of time. The measured V_s of steel slag at a curing time of approximately 0 was slightly smaller than that of gravel. However, the tested steel slag showed 32 % higher V_s than gravel at a curing time of $>$ 18 days, indicating the emergence of a time-dependent stiffness gain owing to the cementation effect.

Han [2] reported that the hydration reaction of calcium oxide (CaO) and magnesium oxide (MgO) in steel slag generates heat, which reduces the moisture content in the steel slag and subsequently increases its strength or stiffness. Additionally, Toda et al. [29] compared the X-ray diffraction (XRD) analysis and scanning electron microscopy (SEM) images of steel slag–dredged soil mixtures and concluded that the calcium and magnesium hydroxides (i.e., hydrated CaO and MgO) can react with silica (SiO_2) and alumina (Al_2O_3) in the slag or surrounding soil to form calcium-silicate-hydrate (C-S-H), calcium-aluminate-hydrate (C-A-H), magnesium-silicate-hydrate (M-S-H), and magnesium-aluminate-hydrate (M-A-H) gels. These gels, particularly C-S-H, are well known for their role in the hardening of cementitious materials [30]. They fill the pores between the steel slag particles, increasing the strength and stiffness over the curing time [29]. Thus, the V_s of the tested steel slag in Fig. 4(b) increased over time, implying that the use of steel slag as fill material or aggregate in compaction piles may have an additional reinforcement effect on the surrounding soils over time due to the cementation effect.

3.2. Field tests

This section analyzes the field test results of Standard Penetration Tests (SPT) and settlement monitoring after the construction of a 2-m high embankment and environmental assessment. SPTs were conducted on both the in-situ soils (inter-pile SPT) and compaction

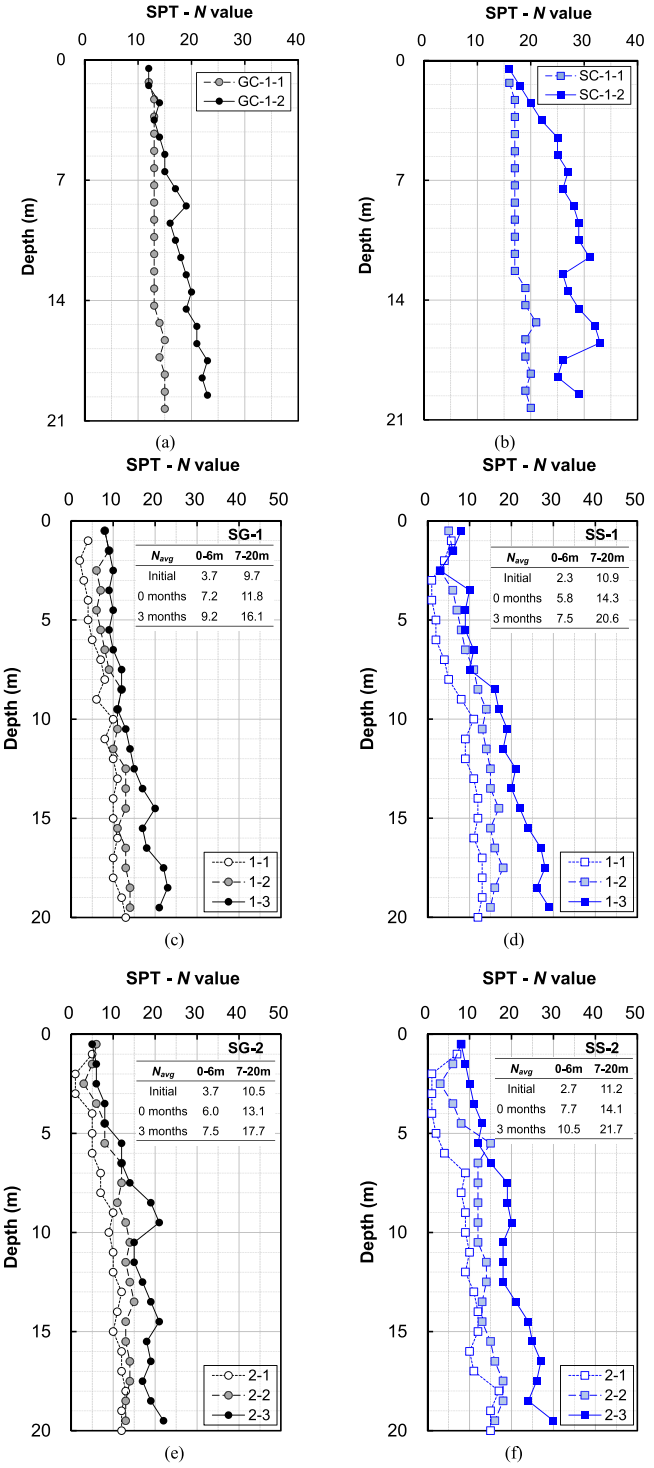

Fig. 5. SPT-*N* values of (a) and (b) in-pile; and (c)–(f) inter-pile before and after pile construction. Note (a), (c) and (e) = gravel compaction pile (GCP); and (b), (d) and (f) = steel slag compaction pile (SSCP).

piles (in-pile SPT) before and immediately after compaction pile construction (0 months after construction). Additionally, this analysis includes supplementary SPT results obtained at the end of settlement monitoring induced by the embankment. The embankment was constructed 0 months after the compaction pile construction, and the settlement was monitored over a 3 month period.

3.2.1. SPT

Fig. 5 shows the results of in-pile and inter-pile SPTs. Note SPTs were performed across three distinct time intervals: before construction (SG-1–1, SG-2–1, SS-1–1, and SS-2–1, where SG = soil reinforced with gravel column and SS = soil reinforced with steel slag column), immediately after construction or 0 months (SG-1–2, SG-2–2, SS-1–2, SS-2–2, GC-1–1, and SC-1–1, where GC = gravel column and SC = steel slag column), and 3 months post-construction (SG-1–3, SG-2–3, SS-1–3, SS-2–3, GC-1–2, and SC-1–2) of both gravel compaction pile (GCP) and steel slag compaction pile (SSCP). Fig. 5 shows that the in-situ soil before the construction of GCP or SSCP exhibited a very loose state with SPT-$N \leq 5$ [31] up to a depth of 6 m.

3.2.1.1. In-pile SPT. Fig. 5(a) and 5(b) show the in-pile SPT N values for the GCP and SSCP columns, respectively. Because the compaction piles were constructed through repeated processes with identical compaction energies, the SPT N on the granular columns showed a fairly uniform distribution along the depth immediately after installation. The slight increase in the SPT N-values observed with increasing depth was due to an increase in the confining stress. It can be observed in Fig. 5(a) and 5(b) that SSCP exhibited approximately 20 % higher SPT- N values than those of the GCP at 0 months (immediately after pile construction). The frictional resistance of steel slag is slightly greater than that of gravel (i.e., the friction angle of steel slag generally ranges from 49° to 71°) [10, 32]. Thus, the slightly higher N values of the SSCP can be attributed to its greater frictional resistance. In addition, the presence of iron in the raw materials of steel slag [33] and a wider range of particle sizes in steel slag may increase resistance against hammer penetration.

Owing to the increased lateral confinement resulting from the densification of the surrounding soils, the SPT- N values of both the GCP and SSCP columns after 3 months were greater than those after 0 months (Fig. 5(a-b)). However, the SSCP column exhibited a significantly larger increase in N values than the GCP column (72 % increase in N value for SSCP versus a 30 % increase in N value for GCP). Given that both compaction piles were subjected to identical fill loading for 3 months, the superior increment in N value for the SSCP can be attributed to the interactions between the surrounding soil and steel slag, as well as the inherent properties of the steel slag. As the evolution of shear wave velocity with time demonstrates, steel slag can show time-dependent strength or stiffness gain,

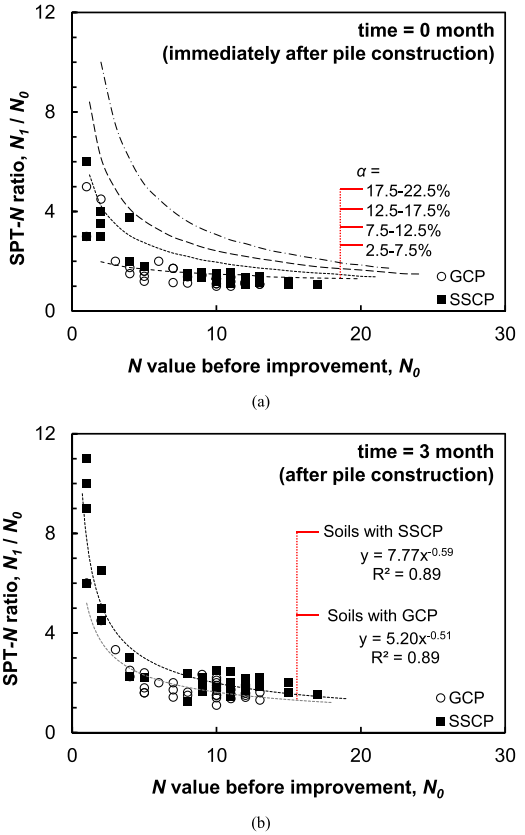

Fig. 6. SPT-N value ratio (N_1/N_0) of reinforced soil at time of (a) 0 months and (b) 3 months after compaction pile construction. Note N_1 = SPT-N values after improvement and N_0 = SPT-N values before improvement.

causing the steel slag column to act as an internally reinforced (or semi-rigid) granular column over time. Consequently, the in-pile SPT- N value of the steel slag column after the completion of the chemical reaction was much greater than that of the gravel column.

3.2.1.2. Inter-pile SPT. Fig. 5(c–f) show that the subsoil before compaction pile construction can be divided into two layers: an upper loose layer (N value ≤ 5) with a depth of 6 m, initially in a loose state, and a bottom layer extending from 7 m to 20 m deep with N values > 5. The average values of N over the soil layer depth (N_{avg}) were calculated and are shown in Fig. 5(c–f). As shown in Fig. 5, N_{avg} increased over time regardless of the fill material type.

Immediately after pile installation, both in-situ soils reinforced with GCP and SSCP exhibited a greater increase in N_{avg} in the upper layer than in the bottom layer (0 months in Fig. 5(c–f)). The insertion of a granular column into in-situ soils using the vibro installation technique induces the horizontal displacement of soils, resulting in the densification of loose soils and changes in stress states [34]. This indicates that a significant enhancement in the strength and stiffness of weaker in-situ soils can be achieved through vertical column construction, which can be attributed to the easier particle rearrangement in loose soils [35]. However, after 3 months of fill loading, a greater change in N_{avg} was measured for the bottom layer. This increase is attributed to the improved load transfer to the deeper soil layer, resulting from densification and the consequent increase in the shear strength of the upper soil layer [36].

3.2.1.3. Quantitative analyses. For a quantitative comparison between soils reinforced with SSCP and GCP, the SPT-N value ratio (N_1/N_0, where $N_1 = N$ value after improvement and $N_0 = N$ value before improvement) is plotted according to N_0 shown in Fig. 6. Note that the SPT-N value ratio is the function of N_0 and area replacement ratio (α), and the trendline given in Han [2] can be approximated according to the following formulas:

$$N_1/N_0 = 2.27 \times {N_0}^{-0.19} \quad \text{when } \alpha = 2.5\% - 7.5\% \tag{1}$$

$$N_1/N_0 = 5.92 \times {N_0}^{-0.48} \quad \text{when } \alpha = 7.5\% - 12.5\% \tag{2}$$

$$N_1/N_0 = 9.20 \times {N_0}^{-0.58} \quad \text{when } \alpha = 12.5\% - 17.5\% \tag{3}$$

$$N_1/N_0 = 16.76 \times {N_0}^{-0.74} \quad \text{when } \alpha = 17.5\% - 22.5\% \tag{4}$$

Fig. 6(a) shows that the variation of N_1/N_0 according to N_0 of soils reinforced with SSCP was comparable to that with GCP at 0 months, indicating that SSCP can show comparable performance with GCP in the short term. However, soils reinforced with SSCP showed greater N_1/N_0 at a given N_0 compared to soils reinforced with GCP at 3 months (Fig. 6(b)), and the relationship between N_1/N_0 and N_0 of soils with SSCP and that with GCP can be expressed as follows:

$$N_1/N_0 = 5.20 \times {N_0}^{-0.51} \text{ for soils with GCP} \tag{5}$$

$$N_1/N_0 = 7.77 \times {N_0}^{-0.59} \text{ for soils with SSCP} \tag{6}$$

Because the α of field tests performed in this study was 12 %, Eqs. (5) and (6) were compared with Eq. (2). Eq. (5) yielded approximately 19 % lower estimate of N_1/N_0 at a given N_0 compared to Eq. (2), whereas Eq. (6) yielded approximately 10 % greater estimate of N_1/N_0, reflecting that both Eqs. (5) and (6) are comparable with Eq. (2) within the permissible error range of ±20 % [2]. This reinforces the reliability of the results reported in this study.

A comparison between Eqs. (5) and (6) (or Fig. 6(b)) indicates that N_1/N_0 for the soils reinforced with SSCP was approximately 30 % greater than that with GCP at a given N_0, highlighting the superior performance of SSCP in soil improvement. Because an increase in N_1/N_0 at a given N_0 indicates an increase in α (Fig. 6), this observation implies that the increase in strength or stiffness of SSCP due to cementation or hydration is analogous to increasing the area replacement ratio of the granular column without cementitious materials.

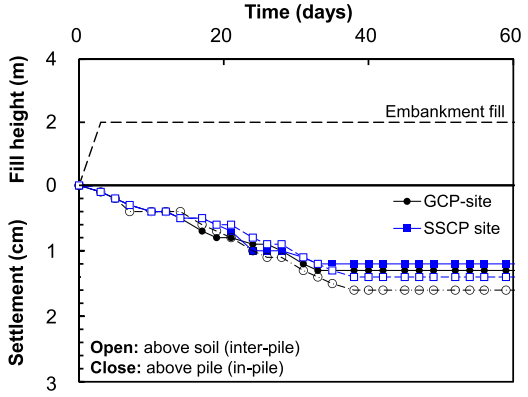

Fig. 7. The measured settlement over time for each composite soil.

The inclusion of chemical binders or geosynthetics in column materials stiffens the column (an internally reinforced column) and increases the load-bearing capacities of the composite grounds [34].

3.2.2. Settlement after embankment (3 months after)

The soils improved with granular columns behave as a composite ground; therefore, to interpret the behavior of the composite ground, including both SSCP and GCP, the settlement was examined following the construction of a 2-m high embankment. Fig. 7 shows the measured settlement over time at two locations, including the embankment fill above the soil (inter-pile) and the embankment fill above the compaction pile (in-pile) at each pile construction area. The settlements appeared to stabilize approximately 35 days after the construction of the embankment.

Similar time-dependent settlements were observed at different measurement locations in both sites; however, the determined stabilized settlement varied slightly according to the location and fill material type: in-pile and inter-pile settlements based on GCP were 1.3 cm and 1.6 cm, respectively; and in-pile and inter-pile settlements based on SSCP were 1.2 cm and 1.4 cm, respectively. These findings indicate that steel slag columns and soils with SSCP were stiffer than gravel columns and soils with GCP, respectively. Additionally, the inter-pile and in-pile settlement difference for GCP was 23 %, and that for SSCP was 17 %, reconfirming that the rigidity (or stiffness) of the steel slag column is greater than that of the gravel column [2,34]. However, the difference in settlement between the granular column and surrounding soil was insignificant, indicating that the tested compaction piles satisfied the equal strain conditions of composite soils with vertical columns [37]. Consequently, the existing theoretical frameworks for sand or gravel compaction pile design remain applicable to the design and behavioral analysis of composite grounds with SSCP.

3.2.3. Environmental impact assessment

Table 2 compares the standard and measured values and provides the results of the environmental assessments, including leaching tests of raw materials (gravel and steel slag), and soil contamination evaluation. The leaching test results show that steel slag, a waste product of the steelmaking industry, meets the hazardous substance standards set by the Waste Management Act of Korea. The gravel also meets these standards; however, the measured heavy metal content in the gravel was slightly higher than that of the steel slag. It is important to note that the gravel used in this study is not a natural geomaterial but crushed aggregate. Therefore, the natural background concentration of heavy metals from the quarry is reflected in the leaching test results of the gravel used in this study.

The summarized values of the heavy metal contents of soils listed in Table 2 represents the maximum measurements taken at five designated locations at constant depths of 5 and 15 m and at three distinct time points: immediately after installation (0 months), 2 months after installation, and 4 months after the installation of compaction piles. The results revealed that soil contamination levels were significantly lower than the regulatory standards for 'Region 1,' with negligible influence from the location and timing of soil sampling.

4. Finite-element analysis

The behavior of composite ground reinforced with steel slag compaction piles (SSCPs) at varying area replacement ratios (α) under the practical stress ranges was evaluated through a finite-element-based numerical program, ABAQUS (Dassault system). Additionally, the impact of steel slag cementation or hydration on composite ground settlement was assessed.

The three-dimensional numerical model was first verified by comparing three Plate Load Test (PLT) results: in-situ soil before pile installation, above the pile (in-pile), and soil between piles (inter-pile) after pile installation. Subsequently, the settlement of composite ground with different α and varying stiffness of SSCPs were assessed by evaluating the response of a circular footing with a diameter (D_{raft}) of 3 m laid above 1 m of sand cushion layer above the composite ground. The details of these models are described in the following section.

4.1. Details of FE modeling

4.1.1. Model geometries

Two different PLTs were simulated before and after the compaction pile construction. For the PLT before pile installation, a circulate plate of diameter of 0.3 m was placed on the native soil. For the PLT after pile installation, the plate was placed on the improved soil and SSCP. Note that the identical pile arrangement shown in Fig. 1(b) was simulated: a total 12 of SSCPs with diameter (D) of 0.7 m and length (L) of 20 m were arranged in 3 rows $\times$ 4 columns with spacing (S) of 1.8 m.

The α of composite ground was controlled by varying numbers and S of SSCPs. The total area of the improved soil, calculated as $S^2 \times$ pile number, was set to twice the area of the circular footing, allowing the footing to cover 50 % of the improved soil region, as shown in Fig. 8. Table 3 lists the α and corresponding pile arrangements covered in this study. Note that only a quarter of the entire model was simulated for the footing above the SSCP-improved soil because the symmetrical behavior of the footing was satisfied.

To minimize the boundary impact on pile behavior, the depth and width of the model were set to exceed 3 L and 5D_{raft} [38]. Fixed and rolling boundary conditions were applied to the bottom and outer planes of the model. For quarter modeling, plane symmetry conditions were applied to the inner planes. A fine mesh geometry was applied to the adjacent elements of the loading area, including the plate and footing. Tie constraints were applied to simulate the interface between the SSCPs and the surrounding soil, considering the tight interlocking between them.

Table 2
Environmental assessment of raw materials and soil contamination.

Components	Leaching of raw materials			Soil contaminations according to time (months)											
	Standard* (mg/L)	Gravel	Steel slag	Standard Region 1** (mg/kg)	GCP site						SSCP site				
					Depth 5 m			Depth 15 m			Depth 5 m			Depth 15 m	
					0	2	4	0	2	4	0	2	4	0	2	4
Arsenic, *As*	1.5	0.07	0	25	8.6	7.5	4.0	7.6	11.2	6.8	7.5	7.6	10.6	7.5	8.2	13.1
Cadmium, *Cd*	0.3	0.01	0	4	0.5	0.6	0.4	0.4	0.4	0.4	0.6	0.5	0.4	0.3	0.4	0.4
Copper, Cu	3	0.4	0.3	150	11	11	17	5	5	13	10	11	18	5	5	17
Hexavalent Chromium, *Cr(VI)*	1.5	0	0	5	0.0	0.0	0.0	0.0	0.0	0.0	0.6	0.0	0.0	0.6	0.0	0.0
Lead, *Pb*	3	0.6	0.1	200	21	22	17	11	12	18	21	23	18	11	12	17
Mercury, *Hg*	0.005	0	0.004	4	0.0	0.0	0.0	0.0	0.0	0.0	0.0	0.0	0.0	0.0	0.0	0.0
Cyanide, *CN*	1	0	0	2	0.0	0.0	0.0	0.0	0.0	0.0	0.0	0.0	0.0	0.0	0.0	0.0
Fluoride, *F*	-	-	-	400	216	209	216	261	246	252	285	216	237	268	257	250
Nickel, *Ni*	-	-	-	100	17	22	15	11	11	18	17	17	14	10	11	9
Zinc, *Zn*	-	-	-	300	56	62	49	40	45	49	58	62	57	40	42	51

*: reference values from Standard Methods for Testing Waste (ES06000, South Korea)
**: reference values from Standard Methods for Testing Soil contamination (ES07000, South Korea)

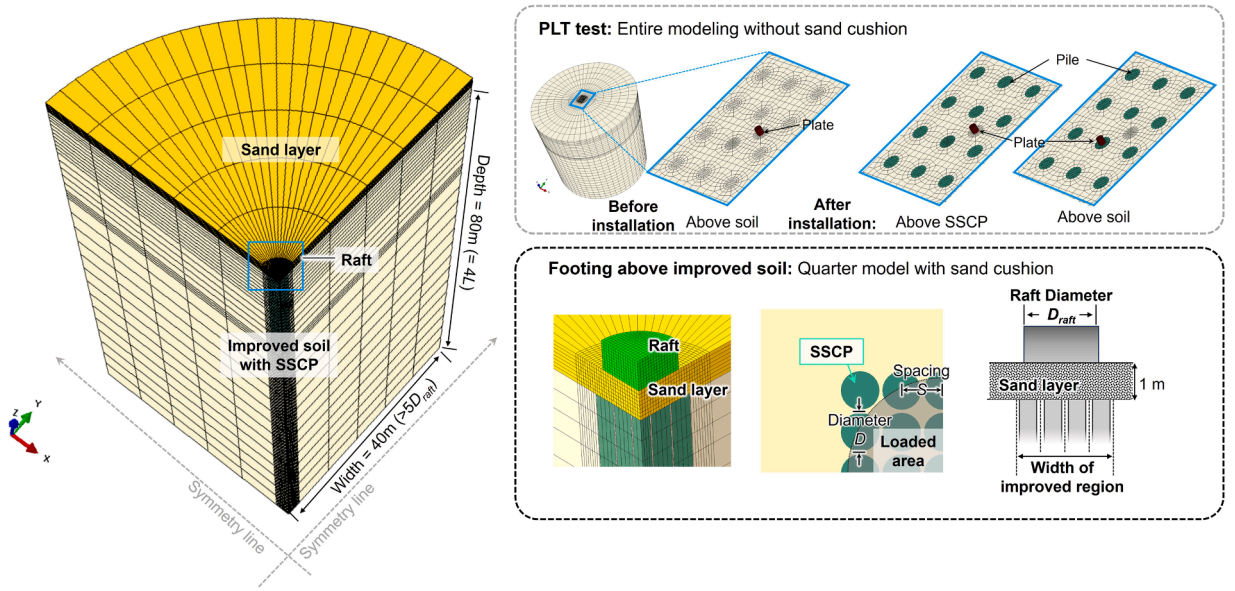

Fig. 8. Model configuration and mesh geometry of the FE model.

Table 3
Area replacement ratio (α) and geometries of compaction pile and raft used in FE modelling.

Replacement ratio, α (%)	**11**	**25**	**44**	**68**
Number of SSCPs	4	9	16	25
Spacing, S (m)	1.88	1.25	0.94	0.75

4.1.2. *Mechanical properties of materials*

The soil was modeled as a linear elastic-perfect plastic material described by the Mohr-Coulomb constitutive model. The drill log data indicate that the soil consisted of three layers before improvement (Fig. 1(c)) and two layers after improvement, excluding the surface sand layer. Accordingly, the soil was modeled to have different material properties for each layer. The clayey sand layer extending over a depth of 9 m was modeled to have a high cohesion of 42 kPa, whereas the sandy layer was modeled to have near–zero cohesion of 1 kPa to facilitate software implementation. The elastic modulus of the soil was set to increase linearly with depth (z) ($E_{soil} = E_0 + k{\cdot}z$, where E_{soil} is the elastic modulus of soil, E_0 is the elastic modulus at the surface ($z = 0$), and k is the modulus increment rate), with different E_0 and k values for each layer to mimic the soil confinement due to soil weight [39]. However, the relatively thin sand layer laid on the surface prior to the improvement was modeled to have a constant elastic modulus over the depth. Table 4 lists the material properties of the subsoil.

Several studies have shown that the movement of steel slag within piles produces unique packing structures, which significantly influence crack initiation, propagation, and the corresponding failure modes [40,41]. Despite these distinct characteristics, it is noteworthy that steel slag exhibits stress-strain behavior comparable to that of natural aggregates [42]. Therefore, in this study, the behavior of steel slag was simulated using a conventional soil constitutive model, focusing on the strain ranges prior to failure.

The behavior of the SSCP was simulated using the linear Drucker-Prager model to account for the volume dilatancy when the material yields in shear [43,44]. This model is dependent on pressure, which indicates that the material becomes stronger as the

Table 4
Material properties used in FE modeling.

Material		Depth	Constitutive model	Unit weight, γ (kN/m^3)	Poisson ratio, ν	Elastic modulus, E (MPa)	Cohesion, c (kPa)	Friction angle, ϕ (°)	Dilatancy angle, ψ (°)
subsoil	Before	0–1 m	Mohr-Coulomb	14	0.25	14	1	32	5
		1–9 m				3+0.8z	42	32	5
		> 9 m				6+2z	1	32	5
	After	0–9 m				7 + 2z	42	32	5
		> 9 m					1		
Sand cushion layer		1 m	Mohr-Coulomb	16	0.25	20	1	32	5
steel slag compaction pile, SSCP			Druker-Prager	18.5	0.3	45 and 100	5	53	15

pressure increases. The steel slag was modeled to have a larger unit weight and dilation angle than the soil, according to previous studies [10]. Accordingly, the cohesion of steel slag was considered to be higher than that of sandy soils because dilation partially induced cohesion and the friction angle was assumed to be 53° [10]. The details of the mechanical properties are listed in Table 4. Two different elastic moduli of the SSCP (E_{SSCP}) were used to examine their cementation.

4.1.3. Loading process

Geostatic conditions were first achieved for soils with and without compaction piles. Note that this study adopted the wished-in installation method and ignored the installation effect of SSCPs on the soil [39,45].

To simulate the PLT, a total stress of 500 kPa was applied in each case after positioning the plate above the soil before and after SSCP installation (inter-pile) and above the SSCP (in-pile). For further settlement analyses with different α and E_{SSCP}, a total stress of 300 kPa (approximately 1 MN) was applied above the footing placed on the composite ground. In particular, the cementation of the SSCP was simulated by varying E_{SSCP} from 45 to 100 MPa as the applied stress on the footing increased from 100 to 160 kPa (E_{SSCP} = 45 MPa at applied stress = 0 – 100kPa and E_{SSCP} = 100 MPa at applied stress > 160 kPa). Therefore, the impact of SSCP cementation on footing settlement under actual field conditions was analyzed. The cementation effect was evaluated at constant $\alpha = 0.44$ to compare with cases of higher α (= 0.68) at a constant E_{SSCP} of 45 MPa.

4.2. Modeling results

4.2.1. Model verification (PLT test)

Fig. 9 compares the simulated PLT results with the measured data for each case: above the soil before and after SSCP installation and above the SSCP. The mean average percentage error (MAPE) for each case indicates that the adopted model provides reasonable information on foundation behavior.

4.2.2. Effects of α

Fig. 10 (a) shows the load-settlement curve of footing on the composite ground with varying α at E_{SSCP} = 45 MPa. As expected, the footing settlement reduced as α increased. Because the settlement of the footing is fundamentally affected by the internal stress response of the SSCP [46], the settlement reduction ratio (*SRR*) and load-sharing ratio (*LSR*) of the SSCPs are compared in Fig. 10 (b). The *SRR* is calculated as the ratio of the settlement of improved soil to that of unimproved soil [34,47]. The *LSR* was calculated as the ratio of the load resisted by the piles to the total applied load. Additionally, Fig. 10 (b) shows the classification according to α ranges: low ($\alpha \leq 30$ %), medium (030 % $< \alpha \leq 50$ %), and high ($\alpha > 50$ %) replacement [22].

Fig. 10 (b) shows that increasing α reduces the settlement of footing, as larger loads were transmitted to compaction piles, resulting in increasing load-bearing capacities of footing [21,48]. As the deformation of the compaction pile induces additional soil densification through radial soil locking, *SRR* decreases with the applied stress (q_a) [49], whereas *LSR* is less sensitive to q_a. Furthermore, the reduction in *SRR* with increasing q_a was more pronounced at low α.

Fig. 10 shows the behavior of footing with varied E_{SSCP}. Note that the load-settlement curve for cases with varied E_{SSCP} showed similar to that of $\alpha = 0.68$ after 100 kPa (Fig. 10 (a)). Fig. 10 (b) shows a significant increase in *LSR* after E_{SSCP} increment (cementation

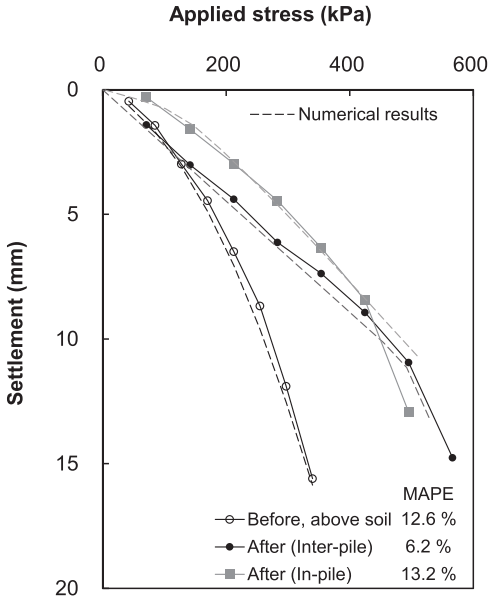

Fig. 9. Load-settlement response of plate load test in case of steel slag compaction piles. Note, MAPE $= \frac{1}{n}\sum_{i=1}^{n}\left|\frac{measured\ value - estimated\ value}{measured\ value}\right|$.

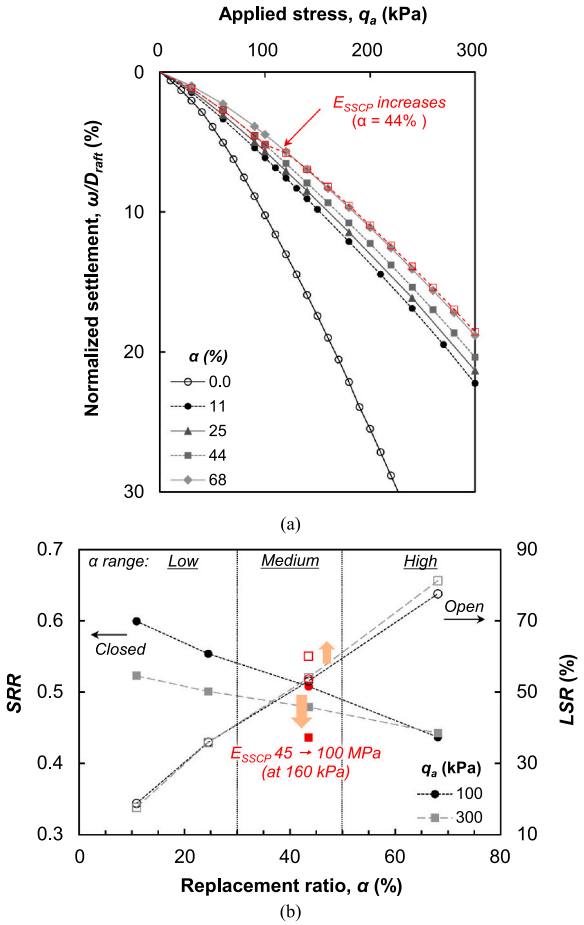

Fig. 10. (a) Load settlement curve of footing according to area replacement ratio (α); and (b) settlement reduction ratio (*SRR*) and load sharing ratio (*LSR*) of footing according to α and applied stress (q_a).

of the compaction pile), which consequently reduced the footing settlement (lower *SRR*) [50,51]. This confirms that the impact of cementation or hydration of compaction fill material has an effect equivalent to that of increasing α, as shown in Fig. 6. Specifically, assuming E_{SSCP} increased by approximately 2.2 times due to steel slag hardening, the cementation effect was equivalent to increasing α by about 1.12 times for load distribution and by 1.64 times for settlement reduction at $q_a = 300$kPa.

5. Summary and conclusions

This study comprehensively evaluates the feasibility of using steel slag produced in South Korea as a fill material or aggregate for compaction piles to improve the engineering properties of soft soils. Through a series of field and laboratory tests, the mechanical performance of steel slag compaction piles (SSCPs) was compared to that of traditional gravel compaction piles (GCPs). Additionally, the environmental stability of the steel slag was confirmed through an environmental impact assessment at the testing site. The key observations made in this study are as follows:

•The cementitious properties of steel slag were confirmed by laboratory testing, which measured shear wave velocities over curing times.

•The Standard Penetration Test (SPT) *N*-ratios (N_1/N_0, where $N_1 = N$ value after improvement and $N_0 = N$ value before improvement) were comparable for soils reinforced with SSCPs and GCPs immediately after installation. However, after 3 months, SSCP-reinforced soils showed approximately 30 % higher N-ratios, which can be attributed to the cementation of the steel slag.

•Numerical analyses validate that the cementation of steel slag has an effect equivalent to increasing the compaction pile replacement ratio (α). Specifically, this study observed that the simulated cementation effect of increasing the compaction pile stiffness by about 2.2 times is equivalent to an increase in α of about 1.12 times for load distribution and about 1.64 times for settlement reduction.

In conclusion, the comprehensive investigation conducted in this study provides strong evidence that steel slag is a viable alternative to conventional gravel as a fill material for compaction piles, offering improved soil stabilization performance and environmental sustainability. The findings of this research can contribute to the development of more sustainable ground improvement

techniques utilizing industrial byproducts, such as steel slag.

CRediT authorship contribution statement

Hyunwook Choo: Writing – review & editing, Investigation, Conceptualization. **Yong Hun Cho:** Methodology, Investigation. **Boyoung Yoon:** Writing – original draft, Investigation, Data curation. **Jaewon Jang:** Investigation, Funding acquisition.

Declaration of Competing Interest

The authors declare that they have no known competing financial interests or personal relationships that could have appeared to influence the work reported in this paper.

Acknowledgements

This research was supported by POSCO research fund (2023A043) and the National Research Foundation of Korea (NRF) grant funded by the Korean government (MSIT). RS-2023–00208844

Appendix A. Supporting information

Supplementary data associated with this article can be found in the online version at doi:10.1016/j.cscm.2024.e03900.

Data Availability

Data will be made available on request.

References

[1] S.S.G. Prasad, Y. Harish, P. Satyanarayana, Stabilization of marine clays with geotextile reinforced stone columns using silica-manganese slag as a stone column material, Int. J. Comput. Eng. Res. 5 (09) (2015) 05–12.
[2] J. Han, Principles and Practice of Ground Improvement, 1st, John Wiley & Sons, 2015.
[3] P. Andreou, W. Frikha, R. Frank, J. Canou, V. Papadopoulos, J.C. Dupla, Experimental study on sand and gravel columns in clay, Proc. Inst. Civ. Eng.-Ground Improv. 161 (4) (2008) 189–198.
[4] V.R. Schaefer, R.R. Berg, B.R. Christopher, J.A. DiMaggio, G.M. Filz, D.A. Bruce, D. Ayala, J.G. Collin, R.R. Berg, Geotechnical Engineering Circular No. 12 Ground Modification Methods-Reference Manual Volume I, National Highway Institute (US),2016.
[5] M. Alamgir, N. Miura, H.B. Poorooshasb, M.R. Madhav, Deformation analysis of soft ground reinforced by columnar inclusions, Comput. Geotech. 18 (4) (1996) 267–290, https://doi.org/10.1016/0266-352X(95)00034-8.
[6] M. Hatanaka, L. Feng, N. Matsumura, H. Yasu, A study on the engineering properties of sand improved by the sand compaction pile method, Soils Found. 48 (1) (2008) 73–85, https://doi.org/10.3208/sandf.48.73.
[7] S.-K. You, J. Lee, M.A. Gabr, Experimental evaluation of recycled aggregate porous concrete piles for soft ground improvement, Mar. Georesour. Geotechnol. 34 (8) (2016) 712–720, https://doi.org/10.1080/1064119X.2015.1076913.
[8] C.J. Serridge, Achieving sustainability in vibro stone column techniques, Proc. Inst. Civ. Eng. Eng. Sustain. (2005) 211–222.
[9] A. Zukri, R. Nazir, Sustainable materials used as stone column filler: a short review, IOP Conf. Ser. Mater. Sci. Eng. 342 (1) (2018) 012001, https://doi.org/10.1088/1757-899X/342/1/012001.
[10] I.Z. Yildirim, M. Prezzi, Geotechnical properties of fresh and aged basic oxygen furnace steel slag, J. Mater. Civ. Eng. 27 (12) (2015) 04015046 http://doi.org/doi:10.1061/(ASCE)MT.1943-5533.0001310.
[11] C. Shi, Steel slag—its production, processing, characteristics, and cementitious properties, J. Mater. Civ. Eng. 16 (3) (2004) 230–236, https://doi.org/10.1061/(ASCE)0899-1561(2004)16:3(230).
[12] USGS, U.S. Geological Survey Mineral Commodity Summaries, 2022.
[13] KOSA, Korea Iron and Steel Association: Steel Slag Recycling Performance in 2022 and Recycling Plan In 2023, 2023.
[14] O. Gencel, O. Karadag, O.H. Oren, T. Bilir, Steel slag and its applications in cement and concrete technology: a review, Constr. Build. Mater. 283 (2021) 122783, https://doi.org/10.1016/j.conbuildmat.2021.122783.
[15] M.J. Rezaei-Hosseinabadi, M. Bayat, B. Nadi, A. Rahimi, Sustainable utilisation of steel slag as granular column for ground improvement in geotechnical projects, Case Stud. Constr. Mater. 17 (2022) e01333, https://doi.org/10.1016/j.cscm.2022.e01333.
[16] Y. Gan, C. Li, W. Ke, Q. Deng, T. Yu, Study on pavement performance of steel slag asphalt mixture based on surface treatment, Case Stud. Constr. Mater. 16 (2022) e01131, https://doi.org/10.1016/j.cscm.2022.e01131.
[17] I. Barišić, I. Netinger Grubeša, B. Hackenberger Kutuzović, Multidisciplinary approach to the environmental impact of steel slag reused in road construction, Road. Mater. Pavement Des. 18 (4) (2017) 897–912, https://doi.org/10.1080/14680629.2016.1197143.
[18] M.J. Rezaei-Hosseinabadi, M. Bayat, B. Nadi, A. Rahimi, Utilisation of steel slag as a granular column to enhance the lateral load capacity of soil, Geomech. Geoengin. 17 (5) (2022) 1406–1416, https://doi.org/10.1080/17486025.2021.1940315.
[19] S.V. Sivapriya, S. Gunalan, A. Mugesh, J. Niranjan, K. Yuvaraj, Investigating the advantage of copper and steel slags as partial replacement material in a sand compaction column in stabilizing the soft clay, Int. J. Geotech. Eng. 17 (5) (2023) 510–518, https://doi.org/10.1080/19386362.2023.2239686.
[20] K. Onda, H. Honda, H. Yoshitake, Examination of application of steel slag to sand compaction pile method, JFE Tech. Rep. 19 (19) (2014) 41–48.
[21] J.T. Shahu, M.R. Madhav, S. Hayashi, Analysis of soft ground-granular pile-granular mat system, Comput. Geotech. 27 (1) (2000) 45–62, https://doi.org/10.1016/S0266-352X(00)00004-5.
[22] M. Kitazume, The Sand Compaction Pile Method, CRC Press, 2005.
[23] D.A. Greenwood, K. Kirsch Specialist, Ground treatment by vibratory and dynamic methods, Piling Ground Treat. (2015) 17–45.
[24] G. Wang, Y. Wang, Z. Gao, Use of steel slag as a granular material: volume expansion prediction and usability criteria, J. Hazard. Mater. 184 (1) (2010) 555–560, https://doi.org/10.1016/j.jhazmat.2010.08.071.

[25] Z.C. Huang, J.C.M. Ho, J. Cui, F.M. Ren, X. Cheng, M.H. Lai, Improving the post-fire behaviour of steel slag coarse aggregate concrete by adding GGBFS, J. Build. Eng. 76 (2023) 107283, https://doi.org/10.1016/j.jobe.2023.107283.
[26] Z. Huang, B. Zhang, J.C.M. Ho, F. Ren, M. Lai, Improving passing ability of ultra-heavy-weight concrete by optimising its packing structure, Mag. Concr. Res. (2024), https://doi.org/10.1680/jmacr.24.00143.
[27] Z.C. Huang, J.J. Liu, F.M. Ren, J. Cui, Z. Song, D.H. Lu, M.H. Lai, Behavior of SSFA high-strength concrete at ambient and after exposure to elevated temperatures, Case Stud. Constr. Mater. 20 (2024) e02946, https://doi.org/10.1016/j.cscm.2024.e02946.
[28] Expansion Test Method of Steel Slag Immersed at 80℃, Korean Agency for Technology and Standards KS F 2580 (2022).
[29] K. Toda, H. Sato, N. Weerakoon, T. Otake, S. Nishimura, T. Sato, Key Factors affecting strength development of steel slag-dredged soil mixtures, Minerals 8 (5) (2018) 174, https://doi.org/10.3390/min8050174.
[30] I.G. Richardson, The nature of C-S-H in hardened cements, Cem. Concr. Res. 29 (8) (1999) 1131–1147, https://doi.org/10.1016/S0008-8846(99)00168-4.
[31] K. Terzaghi, R.B. Peck, G. Mesri, Soil Mechanics in Engineering Practice, John wiley & sons, 1996.
[32] F. Maghool, A. Arulrajah, C. Suksiripattanapong, S. Horpibulsuk, A. Mohajerani, Geotechnical properties of steel slag aggregates: Shear strength and stiffness, Soils Found. 59 (5) (2019) 1591–1601, https://doi.org/10.1016/j.sandf.2019.03.016.
[33] N. Ma, D.G. Hill, L.A. Wood, J.B. Houser, R.W. Lewis, Fast assessment of total iron contents in steelmaking slags by means of water displacement test for recycling of the iron in the ironmaking and steelmaking process, J. Sustain. Met. 3 (3) (2017) 450–458, https://doi.org/10.1007/s40831-017-0127-3.
[34] M.R. Dheerendra Babu, S. Nayak, R. Shivashankar, A critical review of construction, analysis and behaviour of stone columns, Geotech. Geol. Eng. 31 (1) (2013) 1–22, https://doi.org/10.1007/s10706-012-9555-9.
[35] B. Ryu, H. Choo, J. Park, S.E. Burns, Stress–deformation response of rigid–soft particulate mixtures under repetitive Ko loading conditions, Transp. Geotech. 37 (2022) 100835, https://doi.org/10.1016/j.trgeo.2022.100835.
[36] S. Murugesan, K. Rajagopal, Model tests on geosynthetic-encased stone columns, Geosynth. Int. 14 (6) (2007) 346–354, https://doi.org/10.1680/gein.2007.14.6.346.
[37] L. Miao, F. Wang, W. Lv, A simplified calculation method for stress concentration ratio of composite foundation with rigid piles, KSCE J. Civ. Eng. 22 (9) (2018) 3263–3270, https://doi.org/10.1007/s12205-018-1558-5.
[38] A.S. Azizkandi, H. Rasouli, M.H. Baziar, Load sharing and carrying mechanism of piles in non-connected pile rafts using a numerical approach, Int. J. Civ. Eng. 17 (6) (2019) 793–808, https://doi.org/10.1007/s40999-018-0356-2.
[39] F. Tradigo, F. Pisanò, C. Di Prisco, A. Mussi, Non-linear soil–structure interaction in disconnected piled raft foundations, Comput. Geotech. 63 (2015) 121–134, https://doi.org/10.1016/j.compgeo.2014.08.014.
[40] M.H. Lai, Y.W. Liang, Q. Wang, F.M. Ren, M.T. Chen, J.C.M. Ho, A stress-path dependent stress-strain model for FRP-confined concrete, Eng. Struct. 203 (2020) 109824, https://doi.org/10.1016/j.engstruct.2019.109824.
[41] M.H. Lai, J.L. Lin, J. Cui, F.M. Ren, S. Kitipornchai, J.C.M. Ho, A novel packing-coupled stress-strain model for confined concrete, Eng. Struct. 303 (2024) 117415, https://doi.org/10.1016/j.engstruct.2023.117415.
[42] P.K. Chamling, S. Haldar, S. Patra, Physico-chemical and mechanical characterization of steel slag as railway ballast, Indian Geotech. J. 50 (2) (2020) 267–275, https://doi.org/10.1007/s40098-020-00421-7.
[43] M.A. Nav, R. Rahnavard, A. Noorzad, R. Napolitano, Numerical evaluation of the behavior of ordinary and reinforced stone columns, Structures 25 (2020) 481–490, https://doi.org/10.1016/j.istruc.2020.03.021.
[44] H.L. Liu, C.W.W. Ng, K. Fei, Performance of a geogrid-reinforced and pile-supported highway embankment over soft clay: case study, J. Geotech. Geoenviron. 133 (12) (2007) 1483–1493, https://doi.org/10.1061/(ASCE)1090-0241(2007)133:12(1483).
[45] S. Richter, R.O. Cudmani, C. Slominski, The behavior of a spread footing over reinforced ground with gravel interface during a strong earthquake, Geotechnik 34 (3) (2011) 193–204, https://doi.org/10.1002/gete.201000019.
[46] Q. Yang, Z. Li, L.J. Li, L. Song, Comprehensive experimental investigation of improved clay ground by sand compaction pile varying from low to high area replacement ratios, 04023155, Int. J. Geomech. 23 (9) (2023), https://doi.org/10.1061/IJGNAI.GMENG-860.
[47] H. Aboshi, E. Ichimoto, E. M, H. K, The compozer-a method to improve characteristics of soft clay by inclusion of large diameter sand columns, Proc. Int. Conf. Soil Reinf. Reinf. Earth Other Tech. (1979) 211–216.
[48] A.P. Ambily, S.R. Gandhi, Behavior of stone columns based on experimental and FEM analysis, J. Geotech. Geoenviron. 133 (4) (2007) 405–415, http://doi.org/doi:10.1061/(ASCE)1090-0241(2007)133:4(405).
[49] I. Juran, A. Guermazi, Settlement response of soft soils reinforced by compacted sand columns, J. Geotech. Eng. 114 (8) (1988) 930–943, http://doi.org/doi:10.1061/(ASCE)0733-9410(1988)114:8(930).
[50] A.Z. Elwakil, W.R. Azzam, Experimental and numerical study of piled raft system, Alex. Eng. J. 55 (1) (2016) 547–560, https://doi.org/10.1016/j.aej.2015.10.001.
[51] P. Clancy, M. Randolph, Simple design tools for piled raft foundations, Géotechnique 46 (2) (1996) 313–328, https://doi.org/10.1680/geot.1996.46.2.313.